

Early Benefits of Mitigation in Risk of Regional Climate Extremes

Andrew Ciavarella*¹, Peter Stott¹ and Jason Lowe¹

¹Met Office Hadley Centre, FitzRoy Road, Exeter, EX1 3PB, UK

Large differences in climate outcomes are projected by the end of this century depending on whether greenhouse gas (GHG) emissions continue to increase or are reduced sufficiently to limit total warming to below 2°C.¹ However it is generally thought that benefits of mitigation are hidden by internal climate variability until later in the century.² Here we show that if the likelihood of extremely hot seasons is considered, the benefits of mitigation emerge more quickly than previously thought. It takes less than twenty years of emissions reductions in many regions for the likelihood of extreme seasonal warmth to reduce by more than half following initiation of mitigation. Additionally we show that the latest possible date at which the probability of extreme seasonal temperatures will be halved through emissions reductions consistent with the 2°C target is in the 2040s. Exposure to climate risk is therefore reduced markedly and rapidly with substantial reductions of GHG emissions demonstrating that the early mitigation needed to limit eventual warming below potentially dangerous levels benefits societies in the nearer-term not just in the longer-term future.

Future changes in climate depend in part upon emissions to date (so-called climate change commitment) and emissions over the coming decades with an approximately linear relationship between total anthropogenic CO₂ emissions and overall warming.³ The impacts on societies around the globe will depend upon regional exposure and vulnerability to the hazards posed by a changing climate, particularly those related to changing climate extremes.

*andrew.ciavarella@metoffice.gov.uk

26 Coupled climate model simulations together with observations and fundamental physical un-
27 derstanding form the basis for assessment of past and future changes in climate. The generation
28 of models supporting the IPCC’s 5th Assessment Report is phase 5 of the Coupled Model Inter-
29 comparison Project (CMIP5)⁴ comprising simulations of 20thC historical climate and scenarios of
30 21stC climate driven by emissions prescribed in a set of Representative Concentration Pathways
31 (RCPs).⁵ These range from an aggressive mitigation scenario, consistent with the scale of emis-
32 sions needed to likely limit warming to 2°C above pre-industrial levels (RCP 2.6), to a scenario in
33 which emissions continue to increase unchecked by climate mitigation policy (RCP 8.5ⁱ).

34 Indicators of key interest are those such as time of emergence (ToE) at which climate changes in
35 a given emissions scenario become detectable above some baseline variability.⁶ Tropical warming
36 leads to emergence of a regional signal earlier than higher latitudes where, despite greater mag-
37 nitude of expected warming, greater variability and lower signal-to-noise retard ToE by several
38 decades. ToE is sensitive to choice of variable and definition of signal, however. Broadly speaking
39 temperature studies concerning larger spatial scales, earlier baselines and tests for change of the
40 full temperature distribution find emergence has already occurred or is soon to do so^{7,8,9} while
41 later baselines and signal-to-noise type metrics show later emergence.^{6,10}

42 The ToE approach has been adapted to examine the emergence of climate changes between two
43 future emissions scenarios to address the benefits of emissions mitigation. Tebaldi and Friedling-
44 stein¹¹ used CMIP5 models to find dates at which a regionally significant difference in trend
45 in seasonal warming emerges between the aggressive mitigation scenario RCP 2.6 and the high
46 emissions scenario RCP 8.5. This date is not until the middle decades of this century in most con-
47 tinental and sub-continental scale regions of the world. The conclusion was drawn that detection
48 of the benefits of mitigation is thus delayed to this time.

49 The most obvious adverse impacts of climate change however are likely to be felt initially
50 though society’s vulnerabilities to locally rare “extreme events”.¹² Furthermore, extreme events
51 defined by some fixed threshold may see dramatic changes in likelihood upon only small changes in
52 the mean state of the climate.^{9,13,14,15} For example, if a climate variable with normally distributed
53 annual values sees a positive shift in its mean of 0.3 standard deviations (a signal to noise of much
54 less than one) the probability of fixed threshold events originally at a 1 in 20 year return level
55 approximately doubles to 1 in 10 years. For the same shift in the mean, extremes at larger return

ⁱThe scenarios are named according to the resulting median total radiative forcing estimated at 2100.

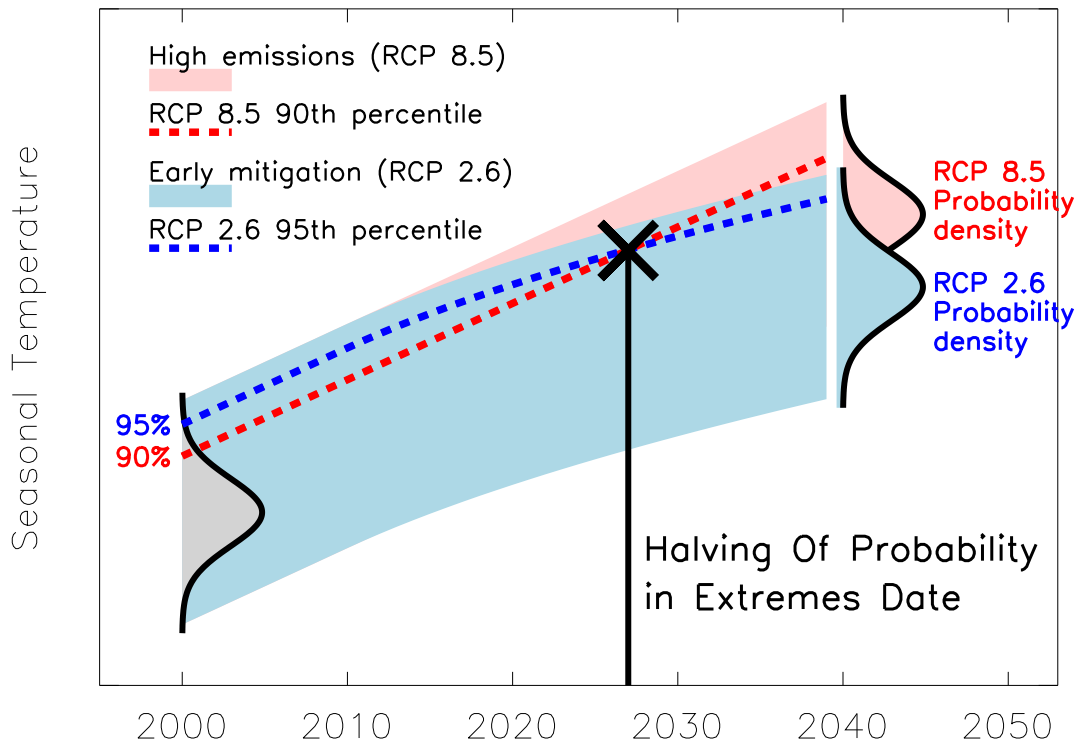


Figure 1: Definition of the Halving of Probability in Extremes Date (HOPE Date). Depicted are idealised non-stationary probability distributions of modelled temperatures and relevant percentiles with time. Distribution widths include contributions to the likelihood from both internal climate variability as well as inter-model uncertainty in response to climate forcings. The grey probability distribution represents a time when emissions scenarios are indistinguishable. Into the 21stC the distribution of seasonal temperatures in a region diverges under different emissions scenarios. The HOPE Date gives an indication of when the likelihood of extreme seasonal warmth in an emissions mitigated world is half that of the same warmth in the unmitigated world.

56 times become more likely by increasingly large factors. This demonstrates the importance of
 57 changes in the expected frequency of extremes before traditional detection is possible and adds
 58 further penalties to delayed emissions reductions.¹⁶

59 This study investigates how quickly benefits of mitigation are realised through reductions in
 60 the risk of extreme temperatures over land. We calculate dates when the modelled likelihood of
 61 regional extreme seasonal warmth in an aggressive mitigation scenario (RCP 2.6) has substantially
 62 decreased compared to its likelihood in an unmitigated scenario (RCP 8.5) as represented through
 63 a multi-model ensemble (MME). We focus on events at 1 in 10 year return levels in the unmitigated
 64 world and calculate the date when they become half as likely, i.e. representing 1 in 20 year return
 65 levels with early mitigation. We call this date the Halving Of Probability in Extremes Date
 66 (HOPE Date), illustrated in Figure 1.

67 Adopting the event attribution paradigm¹⁷ the HOPE Date is the date in a high emissions

68 world beyond which more than 50% of the likelihood of extremes is attributable to the unmitigated
69 component of emissions.

70 Using the 26 SREX regions¹² (Supplementary Information (SI) Figure 1) we focus on local
71 warm seasons, being those in which warm extremes are likely of greatest impact. Despite the
72 relatively large spatial and temporal scale and associated averaging out of more localised, shorter
73 duration extremes, such regions and periods are routinely of interest in attribution studies con-
74 cerning extreme climate events and their impacts.^{18,19}

75 The HOPE Date is the time at which the 90th percentile of the distribution of temperatures
76 under RCP 8.5 is expected to be equal to the 95th percentile under RCP 2.6. With 27 models
77 simulating RCP 2.6 and 8.5 (see SI Table 1) we obtain 58 and 64 member ensembles respectively.
78 The time evolution of percentiles is therefore subject to noise due solely to finite MME size, so
79 Figure 1 is idealised. We largely remove this noise by calculating HOPE Dates from 15-year
80 running means of the raw percentiles; different smoothing periods do not significantly affect the
81 results (SI Figure 2).

82 We address model uncertainty by bootstrapping the MME: for every model included we re-
83 calculate the HOPE Date with all members of this single model removed to produce a range of
84 HOPE Date estimates. We refer to the estimate which includes all available models as the best
85 estimate although we stress the importance of the resulting range.

86 We conduct validation tests on the MME (see Methods), failed by regions where the observa-
87 tions simply do not look like a member of the MME. First we ask for a statistically significant
88 mean correlation between 15-year smoothed observations and MME members over 1905 - 2004 as
89 a check on the timing and sign of response to external forcings. Secondly total time series variance
90 is tested as a check on the consistency of the amplitude of variations (on which our first test is
91 silent) by asking that the observed variance lie within the MME range over the same period. 5
92 of 26 SREX regions (CNA, WAF, CAS, SAS & SAU) fail the first test and two fail the second
93 (AMZ & SAS) leaving 20 regions whose representation of warm seasons by the CMIP5 MME is
94 adequate for the purposes of our analysis.

95 Figure 2 (left hand panels) depicts warm season HOPE Dates calculated for a small selection
96 of regions, repeated for all regions in SI Figure 3. Best estimates are used in panel (a) of Figure
97 3 and column 3 of Table 1. HOPE Dates are found to occur no later than the early 2040s
98 with ranges spanning less than a decade in most regions. Half of SREX regions passing the

99 validation tests see best estimate HOPE Date by 2030. HOPE Dates thus occur considerably
100 sooner (one to two decades) than those typical of RCP-derived mitigation efforts based on a
101 detectable difference in scenario trends.¹¹ The spatial pattern is nevertheless consistent (given
102 quoted uncertainty and for comparable regions and seasons) whereby regions with higher signal
103 to noise in seasonal temperatures emerge first. We would therefore expect HOPE Dates for sub-
104 seasonal temperatures such as dailies and variables with lower signal to noise such as at the grid
105 box scale to be considerably later.

106 RCP inter-scenario emissions diverge significantly from 2010⁵ while to date real world emissions
107 have followed a trajectory much closer to the unmitigated scenario.^{20,21} Therefore such reductions
108 in risk are unlikely to be realisable in practice as early as the RCP 2.6-based HOPE Dates so we
109 next consider replacing RCP 2.6 with delayed mitigation scenarios.

110 It is desirable for delayed mitigation scenarios to warm no more than the existing scenario,
111 RCP 2.6. We therefore calculate latest possible HOPE Dates for hypothetical scenarios with
112 delayed emissions reductions where regional temperatures may experience small overshoots but
113 are constrained to not exceed their peak values under RCP 2.6. This constraint together with the
114 fixed RCP 8.5 reference determines a latest date we may find the HOPE Date, which is hence
115 defined as the date when the smoothed 90th percentile of RCP 8.5 is equal to the peak value
116 of the smoothed 95th percentile of RCP 2.6, as demonstrated in Figure 2 (b), (d), (f) and (h)
117 and SI Figure 4. The results are therefore independent of the detailed mitigation trajectory and
118 avoid scenarios with larger overshoots which Lowe et al.²² show require larger mitigation efforts
119 to return to lower temperatures within century timescales.

120 Correspondingly in Figure 3 (a) we first display the duration between the onset of dramatic
121 emissions reductions (i.e. 2010 in RCP 2.6) and the HOPE Date for all regions passing validation
122 along side the latest possible HOPE Dates in Figure 3 (b), which fall around a decade later than
123 the RCP 2.6-based HOPE Dates themselves (see also Table 1).

124 In panel (d) of Figure 3 we show values of the difference in global annual mean land temper-
125 atures between scenarios, $\Delta T_{\text{land}}^{\text{Global}}$, at the time of the RCP 2.6-derived HOPE Dates as another
126 measure that should possess some scenario independence. Again, the spatial pattern of $\Delta T_{\text{land}}^{\text{Global}}$
127 compares well with the pattern of committed global (land + ocean) warming resulting in emer-
128 gence of local signals above pre-industrial variability found by Mahlstein et al.⁷ where 1°C of
129 global mean annual warming was sufficient to obtain emergence in most countries.

130 Along similar lines a study by Tebaldi et al.²³ finds $\Delta T_{\text{ocean+land}}^{\text{Global}} = 0.4^{\circ}\text{C}$ sufficient for emer-
131 gence of signals in median 20-year smoothed seasonal mean temperatures over half of the land
132 surface. Here we find that by $\Delta T_{\text{land}}^{\text{Global}} = 0.3^{\circ}\text{C}$ between scenarios most regions (15 of 20 passing
133 validation) have already experienced a halving in the risk of warm season extremes. As a land-sea
134 contrast $\Delta T_{\text{land}}^{\text{Global}} / \Delta T_{\text{land+ocean}}^{\text{Global}} > 1$ is a robust feature of simulated and observed warming we
135 conclude that $\Delta T_{\text{land+ocean}}^{\text{Global}} < 0.3^{\circ}\text{C}$ is required for most regions to experience a halving of the
136 probability in warm season extremes.

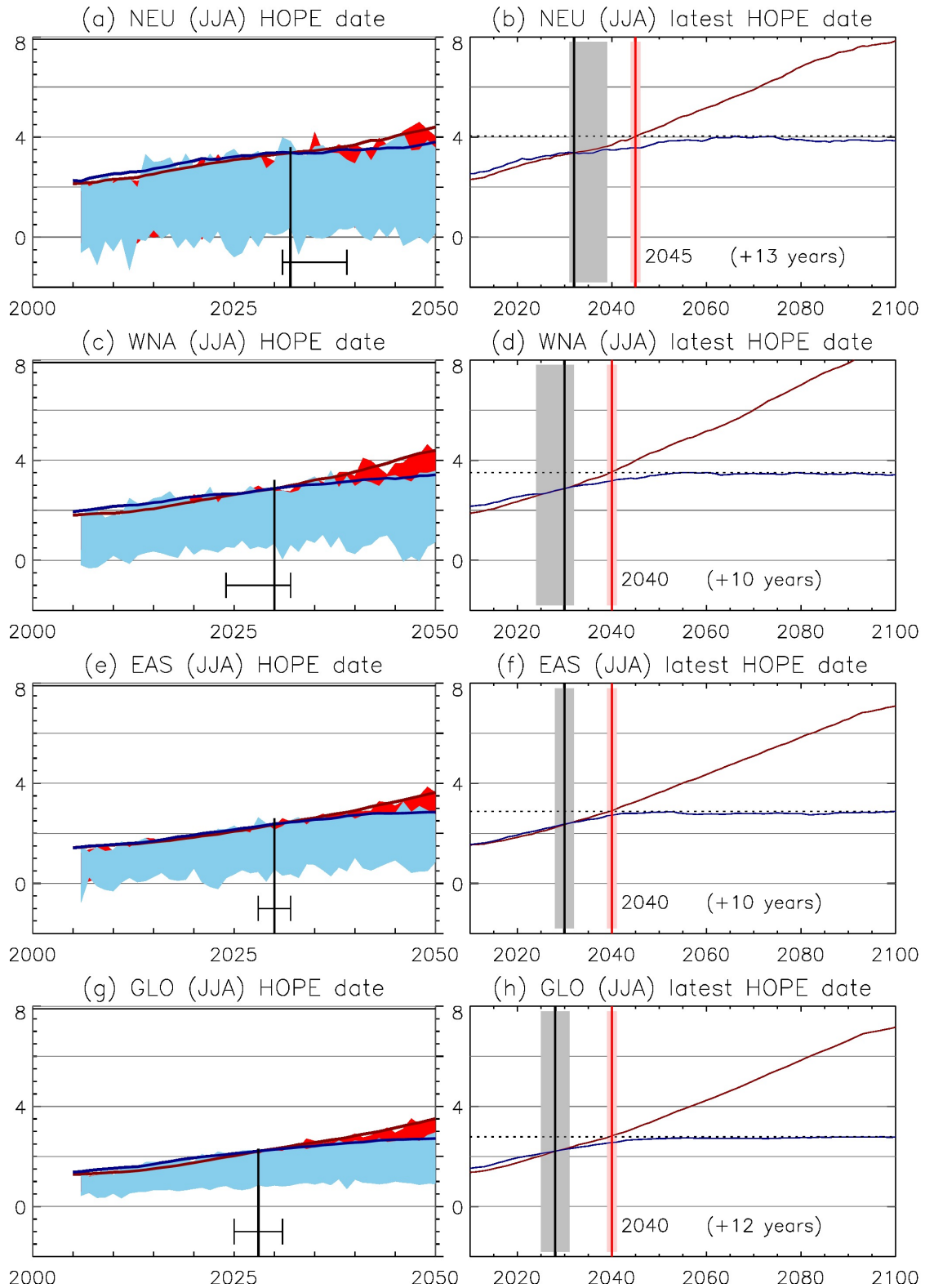


Figure 2: HOPE dates for four selected regions. Left panels show HOPE dates calculated from distributions of regional warm season temperature anomalies (degrees Kelvin with respect to '61-'90 baseline) displayed over 2005 - 2050 from 5 - 95% under RCP 2.6 (early mitigation, light blue) and from 10 - 90% under RCP 8.5 (non-mitigation, red). HOPE Dates are depicted by vertical (best estimate) and horizontal (range) black lines. Right panels show latest possible HOPE dates as determined by the peak value of the 15-year smoothed RCP 2.6 95th percentile, with year stated and delay in years from best estimate HOPE Date in parenthesis. Best estimate HOPE dates are vertical black lines with range in grey, latest possible HOPE dates are vertical red lines with range in pale red. Also plotted in both left and right panels are the relevant 15-year smoothed percentiles (dark blue and dark red correspondingly).

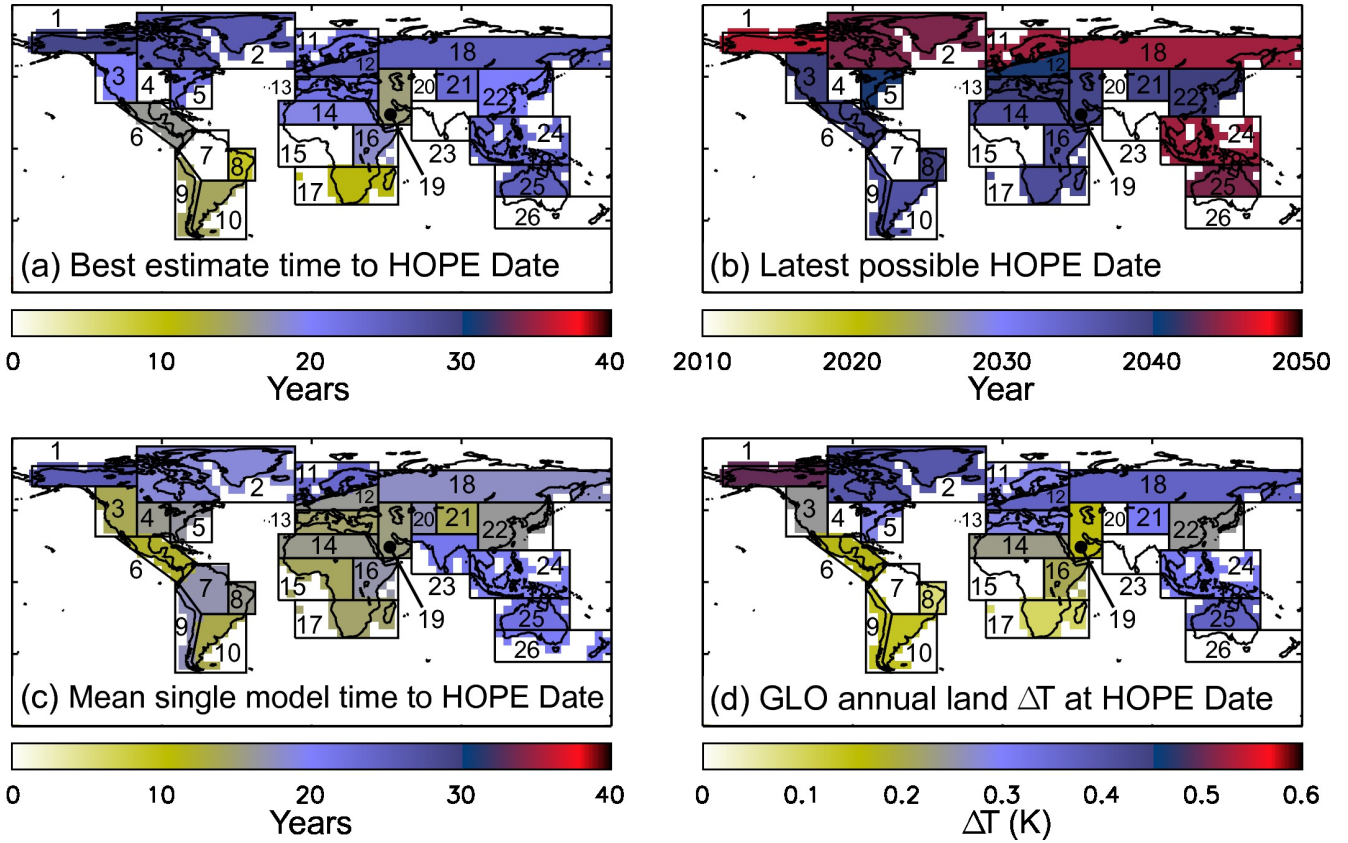


Figure 3: The early benefits of mitigation as represented by regional HOPE Dates. (a) multi-model ensemble (MME) best estimate time between the onset of dramatic emissions reductions (which in RCP 2.6 is 2010) and the HOPE Date when the likelihood of extremes is halved, (b) latest possible HOPE Date itself with onset of emissions reductions delayed from the present and temperatures not exceeding those in the RCP 2.6 scenario, and (c) the mean across single model estimates of the time between the onset of dramatic emissions reductions and the HOPE Date. (d) displays the difference in global mean annual land temperature $\Delta T_{\text{land}}^{\text{Global}}$ between emissions scenario median values at the time of the RCP 2.6 based HOPE Dates implied in panel (a). Regions 4, 7, 15, 20, 23 & 26 fail the MME validation while the remaining 20 regions are adequately represented by the MME for the purposes of the study. HOPE Date ranges can span a couple of years to a decade while ranges of single model estimates can be larger but with the spatial pattern showing broad similarities: an axis north-west to south-east of later dates, including Europe, while Central & South America through Africa and the middle east tend to have earlier dates. Refer to Table 1 and SI Figures 3 - 5 for precise dates and HOPE Date ranges.

137 We additionally investigate model sensitivity by calculating estimates of HOPE Dates from a
 138 selection of individual models (offering RCP ensemble sizes ≥ 3 , see SI), hence removing model
 139 response differences from the probability distributions. Figure 3 (c) shows mean time to HOPE
 140 Dates across models (SI Figure 5 shows the full range). The HOPE Dates thus produced are
 141 consistent with the multi-model values in all regions although the full range of individual model
 142 dates is often as large as two decades. Individual model dates tend to be sooner than MME best
 143 estimates implying that future constraints on warming rates in both scenarios, which effectively
 144 removes ensemble spread due to model response differences, could mean regional HOPE Dates
 145 come sooner than the MME best estimates.

146 Based on this analysis we find that benefits of mitigation through a substantial reduction in
147 the likelihood of extreme seasonal warmth could be felt at regional scales across the world within
148 three decades, even with rapid emissions reductions delayed until 2020 (representing a 10 year
149 delay from the RCP 2.6 scenario). In addition to well known long term benefits provided by early
150 emissions reductions, for example to keep global mean warming below 2°C, our work demonstrates
151 that early mitigation provides short term benefits by reducing exposure to the risks of regional
152 climate extremes.

Region number: name (code)	Warm season	Years until HOPE Date	Latest possible HOPE Date	Validation failure?
8: N. E. Brazil (NEB)	SON	9 [7, 15]	2040 [2039, 2041]	
17: S. Africa (SAF)	DJF	11 [11, 15]	2038 [2037, 2039]	
9: W. Coast South America (WSA)	DJF	14 [8, 17]	2037 [2035, 2038]	
10: S. E. South America (SSA)	DJF	14 [14, 16]	2037 [2036, 2037]	
19: W. Asia (WAS)	JJA	15 [15, 19]	2039 [2038, 2039]	
6: Central America / Mexico (CAM)	JJA	16 [13, 17]	2039 [2037, 2040]	
16: E. Africa (EAF)	MAM	18 [18, 19]	2038 [2035, 2039]	
14: Sahara (SAH)	JJA	19 [16, 20]	2038 [2036, 2040]	
3: W. North America (WNA)	JJA	20 [14, 22]	2040 [2039, 2041]	
22: E. Asia (EAS)	JJA	20 [18, 22]	2040 [2039, 2041]	
5: E. North America (ENA)	JJA	22 [22, 24]	2041 [2040, 2043]	
11: N. Europe (NEU)	JJA	22 [21, 29]	2045 [2044, 2046]	
13: S. Europe / Mediterranean (MED)	JJA	22 [18, 24]	2040 [2040, 2041]	
21: Tibetan Plateau (TIB)	JJA	23 [11, 25]	2039 [2038, 2040]	
24: S. E. Asia (SEA)	MAM	23 [17, 23]	2045 [2044, 2046]	
12: Central Europe (CEU)	JJA	25 [24, 26]	2041 [2041, 2042]	
18: N. Asia (NAS)	JJA	25 [21, 27]	2045 [2044, 2046]	
25: N. Australia (NAU)	DJF	25 [24, 25]	2044 [2043, 2046]	
2: E. Canada / Greenland / Iceland (CGI)	JJA	26 [26, 28]	2044 [2041, 2045]	
1: Alaska / N. W. Canada (ALA)	JJA	29 [26, 29]	2046 [2045, 2047]	
Validation failures				
20: Central Asia (CAS)	JJA	13 [10, 14]	2040 [2037, 2040]	Test 1
26: S. Australia / New Zealand (SAU)	DJF	17 [17, 21]	2040 [2039, 2040]	Test 1
15: W. Africa (WAF)	MAM	18 [12, 19]	2040 [2038, 2041]	Test 1
23: S. Asia (SAS)	JJA	20 [18, 22]	2042 [2039, 2043]	Test 1 & 2
4: Central N. America (CNA)	JJA	23 [22, 23]	2041 [2039, 2041]	Test 1
7: Amazon (AMZ)	SON	30 [19, 31]	2048 [2043, 2049]	Test 2
Continental regions				
31: Africa (regs 14 to 17) (AFR)	MAM	12 [12, 14]	2039 [2037, 2040]	
29: S. America (regs 7 to 10) (SAM)	DJF	17 [14, 18]	2039 [2038, 2040]	
27: Global (all regions) (GLO)	JJA	18 [15, 21]	2040 [2039, 2041]	
32: Asia (regs 18 to 23) (ASI)	JJA	19 [18, 23]	2039 [2037, 2041]	
33: Australasia (regs 24, 25, 26) (AUS)	DJF	19 [17, 19]	2040 [2039, 2042]	
28: N. America (regs 1 to 6) (NAM)	JJA	21 [18, 23]	2040 [2039, 2041]	
30: Europe (regs 11, 12, 13) (EUR)	JJA	22 [21, 25]	2041 [2041, 2042]	

Table 1: Detailed dates, ranges and warm seasons for the regions used in the study. Column three lists the duration in years until the HOPE Date (with model bootstrap ranges described in the text) from the onset of aggressive emissions reductions, which in the mitigation simulations used was in 2010. The fourth column lists the latest possible warm season HOPE Date itself under hypothetical scenarios with emissions reductions delayed beyond the present and temperatures constrained to not exceed their peak under the RCP 2.6 scenario. Validation tests are detailed in the methods and an empty fifth column entry implies both tests were passed.

153 References

- 154 ¹ Collins, M. *et al.* Long-term climate change: projections, commitments and irreversibility
155 (2013).
- 156 ² Kirtman, B. *et al.* Near-term climate change: projections and predictability. *Climate change*
157 953–1028 (2013).
- 158 ³ Allen, M. R. *et al.* Warming caused by cumulative carbon emissions towards the trillionth tonne.
159 *Nature* **458**, 1163–1166 (2009).
- 160 ⁴ Taylor, K. E., Stouffer, R. J. & Meehl, G. A. An overview of cmip5 and the experiment design.
161 *Bulletin of the American Meteorological Society* **93**, 485–498 (2012).
- 162 ⁵ Meinshausen, M. *et al.* The rcp greenhouse gas concentrations and their extensions from 1765
163 to 2300. *Climatic Change* **109**, 213–241 (2011).
- 164 ⁶ Hawkins, E. & Sutton, R. Time of emergence of climate signals. *Geophysical Research Letters*
165 **39** (2012).
- 166 ⁷ Mahlstein, I., Knutti, R., Solomon, S. & Portmann, R. Early onset of significant local warming
167 in low latitude countries. *Environmental Research Letters* **6**, 034009 (2011).
- 168 ⁸ Irina Mahlstein, Gabriele Hegerl, and Susan Solomon. Emerging local warming signals in ob-
169 servational data. *Geophysical Research Letters*, 39(21), 2012.
- 170 ⁹ Andrew D King, Markus G Donat, Erich M Fischer, Ed Hawkins, Lisa V Alexander, David J
171 Karoly, Andrea J Dittus, Sophie C Lewis, and Sarah E Perkins. The timing of anthropogenic
172 emergence in simulated climate extremes. *Environmental Research Letters*, 10(9):094015, 2015.
- 173 ¹⁰ Diffenbaugh, N. S. & Scherer, M. Observational and model evidence of global emergence of
174 permanent, unprecedented heat in the 20th and 21st centuries. *Climatic Change* **107**, 615–624
175 (2011).
- 176 ¹¹ Tebaldi, C. & Friedlingstein, P. Delayed detection of climate mitigation benefits due to climate
177 inertia and variability. *Proceedings of the National Academy of Sciences* **110**, 17229–17234
178 (2013).

- 179 ¹² Field, C. B. *Managing the risks of extreme events and disasters to advance climate change adap-*
180 *tation: special report of the intergovernmental panel on climate change* (Cambridge University
181 Press, 2012).
- 182 ¹³ Christidis, N., Jones, G. S. & Stott, P. A. Dramatically increasing chance of extremely hot
183 summers since the 2003 european heatwave. *Nature Climate Change* (2014).
- 184 ¹⁴ Russo, S., Sillmann, J. & Fischer, E. M. Top ten european heatwaves since 1950 and their
185 occurrence in the coming decades. *Environmental Research Letters* **10**, 124003 (2015).
- 186 ¹⁵ Sanderson, B. M., Oleson, K. W., Strand, W. G., Lehner, F. & O'Neill, B. C. A new ensemble
187 of gcm simulations to assess avoided impacts in a climate mitigation scenario. *Climatic Change*
188 1–16 (2015).
- 189 ¹⁶ Allen, M. R. & Stocker, T. F. Impact of delay in reducing carbon dioxide emissions. *Nature*
190 *Climate Change* **4**, 23–26 (2014).
- 191 ¹⁷ Allen, M. Liability for climate change. *Nature* **421**, 891–892 (2003).
- 192 ¹⁸ Herring, S. C., Hoerling, M. P., Peterson, T. C. & Stott, P. A. Explaining extreme events of
193 2013 from a climate perspective. *Bulletin of the American Meteorological Society* **95**, S1–S104
194 (2014).
- 195 ¹⁹ Herring, S. C., Hoerling, M. P., Kossin, J. P., Peterson, T. C. & Stott, P. A. Explaining extreme
196 events of 2014 from a climate perspective. *Bulletin of the American Meteorological Society* **96**,
197 S1–S172 (2015).
- 198 ²⁰ Peters, G. P. *et al.* The challenge to keep global warming below 2 c. *Nature Climate Change* **3**,
199 4–6 (2013).
- 200 ²¹ Friedlingstein, P. *et al.* Persistent growth of co2 emissions and implications for reaching climate
201 targets. *Nature geoscience* **7**, 709–715 (2014).
- 202 ²² JA Lowe, C Huntingford, SCB Raper, CD Jones, SK Liddicoat, and LK Gohar. How difficult
203 is it to recover from dangerous levels of global warming? *Environmental Research Letters*,
204 4(1):014012, 2009.

205 ²³ Claudia Tebaldi, Brian O’Neill, and Jean-Francois Lamarque. Sensitivity of regional climate to
206 global temperature and forcing. *Environmental Research Letters*, 10(7):074001, 2015.

207 **Corresponding author**

208 Correspondence and requests for materials associated with this article should be directed to An-
209 drew Ciavarella.

210

211 **Acknowledgements**

212 This work was supported by the Joint UK BEIS/Defra Met Office Hadley Centre Climate Pro-
213 gramme (GA01101) and by the EUCLEIA project funded by the European Unions Seventh Frame-
214 work Programme [FP7/20072013] under grant agreement no. 607085. We acknowledge the World
215 Climate Research Programme’s Working Group on Coupled Modelling, which is responsible for
216 CMIP, and we thank the climate modeling groups (listed in SI Table 1) for producing and making
217 available their model output. For CMIP the U.S. Department of Energy’s Program for Climate
218 Model Diagnosis and Intercomparison provides coordinating support and led development of soft-
219 ware infrastructure in partnership with the Global Organization for Earth System Science Portals.

220

221 **Author contributions**

222 AC conducted the research and wrote the first draft of the paper. PS initially suggested a study
223 concerning changing extremes under mitigation. Both PS and JL contributed to discussion of the
224 results and revisions of the paper.

225

226 **Competing financial interests**

227 The authors declare no competing financial interests.

228

229 **Methods**

230

231 The full CMIP5 archive provides 60 climate models from over 20 institutions contributing
232 between 1 and 10 simulations per experiment type, including the 20thC historical experiment and
233 future scenarios RCP 2.6 and RCP 8.5. We use 27 of these models taking simulations differing
234 only through their initial conditions. See SI Table 1 for the full model list and number of members
235 used per experiment.

236 To arrive at the two percentile time series from which the HOPE Date is found we require
237 MME cumulative probability distribution functions (CDFs) at each year, found as follows.

238 Monthly mean fields are first converted to anomalies with respect to 1961 - 1990 at each cell
239 by subtracting the climatological month mean calculated from that ensemble member. Fields are
240 masked using the native resolution model land fraction mask (in three cases where the mask was
241 unavailable that of another model of identical horizontal resolution), removing data in cells with
242 land fraction < 0.25 . We then regrid to $5^\circ \times 5^\circ$ resolution before masking with the spatiotemporal
243 observational coverage of CRUTEM4,²⁴ which after the present uses mean coverage of the final
244 decade of observations (applying a temporal missing data tolerance of 50% of months at each
245 cell). Anomalies are taken again with respect to the same period to avoid distortions introduced
246 upon regridding (again applying a missing data tolerance of 50%) and the resulting data are then
247 closely comparable with the observations used in the validation. We mask CRUTEM4 with land
248 fractions (≥ 0.25) used in the construction of the HadCRUT4 data set.²⁵

249 Seasonal mean fields are then produced (using seasons DJF, MAM, JJA, SON), retaining data
250 in cells where all three months are present. Regional area weighted averages are taken to produce
251 each time series using the masks depicted in SI Figure 1. Continental regions use the combined
252 masks of regions indicated in Table 1 while the GLO region uses the combination of all masks,
253 which hence excludes Antarctica.

254 Regional warm seasons are found by obtaining seasonal means of absolute near surface air
255 temperatures from CRU CL version 2.0²⁷ then taking regional means.

256 The MME empirical CDF for each season is obtained by ranking values at that year in ascend-
257 ing order and assigning each a weight such that the sum over weights is normalised to one and
258 each model is weighted equally (regardless of the number of simulations contributed by a model).
259 The form of the weights assigned to member j of model α used in calculating seasonal CDFs is
260 therefore of the form

$$w_{\alpha j} = \frac{1}{N_\alpha M} \quad (1)$$

261 where N_α is the number of members contributed by model α and M is the number of models.
262 The weights satisfy

$$\sum_{\alpha}^M \sum_j^{N_\alpha} w_{\alpha j} = 1. \quad (2)$$

263 After ordering weights according to their corresponding ranked values the temperature value

264 of percentile $100p$ ($0 < p \leq 1$) may be found as the value at which the sum over the ordered
265 weights up to that corresponding to this value is equal to p . Our method is very similar to that
266 used in a recent study.²⁶ A small difference is that instead of adopting the temperature value of
267 the ensemble member lying closest to the percentile of interest we linearly interpolate between
268 the two nearest values. The value of the 100th percentile is defined to be equal to that of the
269 highest member and the 0th to that of the lowest (which is therefore coincident with the value
270 corresponding to the lowest weight).

271 We are interested in the time when the 95th percentile of RCP 2.6 passes below the 90th
272 percentile of RCP 8.5. Noise due to the finite ensemble size means that percentile series may
273 cross one another several times before separating clearly (a similar issue is discussed in a different
274 context by Hawkins et al., 2014²⁸), biasing HOPE Dates artificially late. To address this we
275 smooth the percentile series using a 15-year box-car window and define the HOPE Date as the
276 final year that the smoothed 95th percentile of RCP 2.6 is greater than smoothed 90th percentile
277 of RCP 8.5.

278 Note that smoothing of percentile series does not reduce the width of the MME distribution.
279 This width represents both inter-annual variability within each model and the component of inter-
280 model spread which incorporates uncertainty in response to external forcings.

281 Bootstrap re-sampling of the MME is performed by removing all members associated with
282 a single model at a time and recalculating weights and percentiles of the MME accordingly. In
283 calculating ranges of latest possible HOPE Dates we simply replace the peak smoothed percentile
284 value with each of its bootstrapped alternatives.

285 Single model HOPE Dates are found by the same method but with only a handful of members
286 per model we instead find percentiles by assuming that single model ensemble members $x(t)$ are
287 generated at time t by a normal stochastic process with variance σ^2 superimposed on the 15-
288 year smoothed empirical model mean $\bar{x}(t)$. σ^2 is calculated from the residuals $r(t) = x(t) - \bar{x}(t)$
289 aggregated across model members and years in the period 2006 - 2099. We required a model have
290 at least 3 ensemble members in each scenario in order that the ensemble mean be sufficiently free
291 of internal variations. This leaves 9 models (see SI Table 1) across which the means displayed in
292 Figure 3 (c) are taken.

293 Annual global mean land temperature difference values, $\Delta T_{\text{land}}^{\text{Global}}$, which appear in Figure 3
294 (d) are calculated from differences between scenario multi-model mean annual anomalies for the

295 GLO region produced by the mean over the four seasonal multi-model median values produced
296 by the same method described above.

297 In the absence of observations from the future with which to validate model responses to
298 future scenario forcings (let alone two possible futures) we assess the performance of the MME
299 against 20thC observations from CRUTEM4.4.0.0.²⁴ We acknowledge that we cannot expect this
300 to be an entirely adequate means of judging model performance into the 21stC as, for example,
301 forcings that cancel one another in an earlier period may fail to do so into the future leading to
302 disguised model deficiencies.^{26,29} We shall adopt the following simple and objective validation
303 paradigm: the MME will be considered adequate in a given region and season if we cannot tell
304 the observational series from a member of the MME itself. As such we require that the MME of
305 historical experiments pass two simple tests.

306 First (Test 1) we assess the timing and relative magnitude of 20th C variability (1905 - 2004)
307 through a comparison of the mean correlation coefficient $\langle r \rangle$ between the 15-yr rolling means of the
308 observed time series and members of the MME with values of r arising between the observations
309 and an isospectral test ensemble, i.e. an ensemble generated by a random process sharing the
310 same power spectrum as the true model ensemble. The test ensemble will have zero mean trend
311 but individual members will look rather like historical series but for trends occurring at different
312 (random) times. A regional warm season fails this test if we cannot rule out that $\langle r \rangle$ could be
313 generated by this random process with high probability.

314

315 H_0 : The mean value of the correlation coefficient, $\langle r \rangle$, between 15-year means of the observed
316 time series and each historical ensemble member can be generated with high probability, p , by a
317 random process isospectral to the true CMIP5 MME.

318

319 We seek to rule out H_0 at the 5% level and fail a regional warm season if we cannot. The
320 isospectral test ensemble contains 10,000 members and upon regeneration produces p values that
321 are robust to within a percent.

322 Secondly (Test 2) we assess the total time series variance of 20thC simulations (also 1905 -
323 2004) across the ensemble by comparison with the total 20thC variance of the observed time series
324 (without any smoothing). A regional warm season fails this test if the observed total variance
325 falls outside the full model range of total variances.

326 Members of the isospectral test ensemble are created as follows. Each member is constructed as
327 a Fourier series in which the phases are selected from a uniform random distribution $U[0, 2\pi]$ while
328 the coefficients at each frequency are selected at random from among the empirical distribution
329 of values obtained from a Fourier decomposition of each member of the true MME. At a given
330 frequency each empirical coefficient will likely be selected many times over in the construction of
331 many test members but the same combination of coefficients across the frequencies is very unlikely
332 to be selected in an ensemble of only 10,000 test members so that the spectrum of each member
333 is very likely unique in addition to possessing random phases. The resulting test ensemble Fourier
334 spectrum will be virtually indistinguishable from the CMIP5 empirical spectrum represented by
335 shaded colours in SI Figure 7.

336 Test 2 assesses the overall scale of variability to which Test 1 is blind.

337 Note that model series are not detrended prior to examining the correlation with observations,
338 power spectra or total variance. This is because we wish to test the relative magnitude and timing
339 of forced responses rather than remove them; we are not attempting to isolate internal variability.

340 SI Figure 6 displays the warm season historical model and observational time series together
341 with Test 1 results. Out of 26 SREX regions 21 pass this test as well as all 6 continents and
342 the global combination. Most regions have $\langle r \rangle \geq 0.6$, many with p values of 1% or better. The
343 continental and GLO region have $\langle r \rangle$ values higher still, all with significance values of 1% or better.
344 While a failure such as 15. WAF (MAM) may be suspected from casual examination of the time
345 series (poor correlation will arise from differing trends in each half of the century) other failures
346 would not be clear, emphasising the need for an objective criterion.

347 SI Figure 7 displays the warm season historical model and observational Fourier spectra with
348 Test 2 results. Two regions fail the total variance test in their warm season: 7. AMZ (SON) and
349 23. SAS (JJA), both of which have observed total variances that fall below every member of the
350 MME. We note that the observed total variance falls close to the bottom of the model range in
351 more than half of the SREX regions and 3 out of 6 continents however.

352

353 **Data availability** The model data supporting this study is available in a public repository, for
354 example at <http://cmip-pcmdi.llnl.gov/cmip5/>. The Met Office observational dataset CRUTEM4
355 is publically available from <http://www.metoffice.gov.uk/hadobs/>.

356

357 References

- 358 ²⁴ PD Jones, DH Lister, TJ Osborn, C Harpham, M Salmon, and CP Morice. Hemispheric and
359 large-scale land-surface air temperature variations: An extensive revision and an update to 2010.
360 *Journal of Geophysical Research: Atmospheres (1984–2012)*, 117(D5), 2012.
- 361 ²⁵ Colin P Morice, John J Kennedy, Nick A Rayner, and Phil D Jones. Quantifying uncertainties
362 in global and regional temperature change using an ensemble of observational estimates: The
363 hadcrut4 data set. *Journal of Geophysical Research: Atmospheres (1984–2012)*, 117(D8), 2012.
- 364 ²⁶ Gareth S Jones, Peter A Stott, and Nikolaos Christidis. Attribution of observed historical near-
365 surface temperature variations to anthropogenic and natural causes using cmip5 simulations.
366 *Journal of Geophysical Research: Atmospheres*, 118(10):4001–4024, 2013.
- 367 ²⁷ Mark New, David Lister, Mike Hulme, and Ian Makin. A high-resolution data set of surface
368 climate over global land areas. *Climate research*, 21(1):1–25, 2002.
- 369 ²⁸ Ed Hawkins, Bruce Anderson, Noah Diffenbaugh, Irina Mahlstein, Richard Betts, Gabi Hegerl,
370 Manoj Joshi, Reto Knutti, Doug McNeall, Susan Solomon, et al. Uncertainties in the timing of
371 unprecedented climates. *Nature*, 511(7507):E3–E5, 2014.
- 372 ²⁹ Piers M Forster, Timothy Andrews, Peter Good, Jonathan M Gregory, Lawrence S Jackson, and
373 Mark Zelinka. Evaluating adjusted forcing and model spread for historical and future scenarios
374 in the cmip5 generation of climate models. *Journal of Geophysical Research: Atmospheres*,
375 118(3):1139–1150, 2013.